Published in final edited form as:
*J Immunol*. 2007 June 1; 178(11): 7072–7080.

# C57BL/6 Mice Genetically Deficient in IL-12/IL-23 and IFN-γ Are Susceptible to Experimental Autoimmune Myasthenia Gravis, Suggesting a Pathogenic Role of Non-Th1 Cells[1]

**Wei Wang**[*,2], **Monica Milani**[*], **Norma Ostlie**[*], **David Okita**[*], **Rajeev K. Agarwal**[†], **Rachel Caspi**[†], and **Bianca M. Conti-Fine**[*,3]

[*] Department of Biochemistry, Molecular Biology and Biophysics, University of Minnesota, Minneapolis, MN 55455

[†] Laboratory of Immunology, National Eye Institute, National Institutes of Health, Bethesda, MD 20892

## Abstract

Immunization with *Torpedo* acetylcholine receptor (TAChR) induces experimental autoimmune myasthenia gravis (EAMG) in C57BL/6 (B6) mice. EAMG development needs IL-12, which drives differentiation of Th1 cells. The role of IFN-γ, an important Th1 effector, is not clear and that of IL-17, a proinflammatory cytokine produced by Th17 cells, is unknown. In this study, we examined the effect of simultaneous absence of IL-12 and IFN-γ on EAMG susceptibility, using null mutant B6 mice for the genes of both the IL-12/IL-23 p40 subunit and IFN-γ (dKO mice). Wild-type (WT) B6 mice served as control for EAMG induction. All mice were immunized with TAChR in Freund's adjuvant. dKO mice developed weaker anti-TAChR $CD4^+$T cells and Ab responses than WT mice. Yet, they developed EAMG symptoms, anti-mouse acetylcholine receptor (AChR) Ab, and $CD4^+$ T cell responses against mouse AChR sequences similar to those of WT mice. dKO and WT mice had similarly reduced AChR content in their muscles, and IgG and complement at the neuromuscular junction. Naive dKO mice had significantly fewer NK, NKT, and $CD4^+CD25^+Foxp3^+$ T regulatory (Treg) cells than naive WT mice. Treg cells from TAChR-immunized dKO mice had significantly less suppressive activity in vitro than Treg cells from TAChR-immunized WT mice. In contrast, TAChR-specific $CD4^+$ T cells from TAChR-immunized dKO and WT mice secreted comparable amounts of IL-17 after stimulation in vitro with TAChR. The susceptibility of dKO mice to EAMG may be due to reduced Treg function, in the presence of a normal function of pathogenic Th17 cells.

---

Cytokines influence the development and modulation of autoimmune responses. Most cytokines are synthesized by and act on a variety of cells. Moreover, they may influence the synthesis and/or activity of other cytokines, directly or indirectly. Because of the complex, pleiotropic, and redundant signaling through the cytokine network, cytokines have complex and at times even contrasting effects on both normal and autoimmune responses.

---

[1]This work was supported by National Institute of Neurological and Communicative Disorders and Stroke Grant NS23919 (to B.M.C.-F.).

2Address correspondence and reprint requests to Dr. Wei Wang, Department of Biochemistry, Molecular Biology and Biophisic, University of Minnesota, 6/155 Jackson Hall, 321 Church Street, Minneapolis, MN 55455. wangx241@umn.edu.

[3]Bianca M. Conti-Fine was previously known as Bianca M. Conti-Tronconi.

**Disclosures**

The authors have no financial conflict of interest.

Many cytokines are growth and differentiation factors or effector molecules of $CD4^+$ T cells. Differentiated $CD4^+$ T cells can be classified into different subsets based on the cytokines they secrete (1–2): The Th1 subset secretes proinflammatory cytokines, such as IFN-$\gamma$ and IL-2, which activate APC and in mice stimulate the synthesis by B cells of IgG that fix complement. Th1 cells can be cytotoxic and are involved in cell-mediated immune responses. The Th2 subset secretes anti-inflammatory cytokines (e.g., IL-4, IL-5, IL-13), which also stimulate humoral immune responses. In mice, Th2 cytokines promote the secretion of IgE and IgG1, which do not fix complement. The Th3 subset secretes TGF-$\beta$ and is involved in immunosuppressive mechanisms. Th17 cells secrete IL-17, a proinflammatory cytokine that is involved in the pathogenesis of several experimental autoimmune diseases (1–3). Other $CD4^+$ T cell subsets have been identified: among them, the $CD4^+CD25^+$ T regulatory (Treg)[4] cells are especially important in maintaining self-tolerance and inhibiting the development of autoimmunity (4).

Myasthenia gravis (MG) and its experimental model, experimental autoimmune myasthenia gravis (EAMG), are Ab-mediated, T cell-dependent autoimmune diseases. Their symptoms are caused by high-affinity IgG against the muscle acetylcholine receptor (AChR) at the NMJ (5,6). EAMG can be induced in mice and other experimental animals by immunization with AChR (7,8). In both MG and rodent EAMG, synthesis of pathogenic anti-AChR Ab requires $CD4^+$ T cells (5,6).

Th1 cells are necessary for EAMG development and IL-12, the major growth and differentiation factor for Th1 cells, has a crucial role for development of mouse EAMG. Wild-type (WT) B6 mice treated with exogenous IL-12 during TAChR immunization developed EAMG earlier, and synthesized more IFN-$\gamma$ and anti-TAChR IgG2a than IL-12 untreated mice (9). Also, BALB/c mice genetically deficient in STAT4 transcription factor, which is crucial for IL-12 intracellular signaling, were EAMG resistant (10). Moreover, B6 mice carrying a disrupted gene for the common p40 subunit shared by both IL-12 and IL-23, and therefore were genetically deficient in both IL-12 and IL-23 (IL-12/IL-$23^{-/-}$ mice), were resistant to EAMG after TAChR immunization (9,11): those studies confirmed the importance of Th1 cells from EAMG development, although they did not dissociate possible distinct roles of IL-12 and IL-23 in this model disease.

The role in EAMG of the Th1 effector cytokine, IFN-$\gamma$, is unclear. In one study, B6 mice genetically deficient in IFN-$\gamma$ (IFN-$\gamma^{-/-}$ mice) were as susceptible to EAMG as WT B6 mice (11): IFN-$\gamma^{-/-}$ and WT mice had comparable concentrations of anti-AChR Ab, and both had IgG and complement at the NMJ (11). Other studies found that mice genetically deficient in IFN-$\gamma$ or IFN-$\gamma$ receptor were less susceptible to EAMG than WT mice and produced less anti-AChR Ab (12,13).

Th17 cells are important in the pathogenesis of several experimental autoimmune diseases. Development of experimental autoimmune encephalomyelitis (EAE) was significantly suppressed in IL-$17^{-/-}$ mice (2); vaccination against IL-17 suppressed collagen-induced arthritis and EAE (14,15); and in experimental autoimmune uveitis, neutralizing IL-17 inhibited disease in WT mice (D. Luger and R. R. Caspi, submitted for publication). A pathogenic role of Th17 cells could explain the susceptibility to autoimmunity in animal models that lack Th1 cells (2,14,16,17).

In this study, we have used dKO B6 mice to investigate the effect of simultaneous absence of both IL-12/IL-23 and IFN-$\gamma$ on EAMG development.

[4]Abbreviations used in this paper: Treg, T regulatory; AChR, acetylcholine receptor; MG, myasthenia gravis; EAMG, experimental autoimmune myasthenia gravis: EAMG; $^{125}$I-$\alpha$ BTX, $^{125}$I-$\alpha$ bungarotoxin; NMJ, neuromuscular junction; SI, stimulation index; TAChR, *Torpedo* AChR; WT, wild type; FoxP3, forkhead box P3.

## Materials and Methods

### Induction and clinical assessment of EAMG

**Mice—**Eight- to 10-wk-old female B6 mice were purchased from The Jackson Laboratory. Mice genetically deficient in IL-12/IL-23 and IFN-$\gamma$ (dKO mice) were generated as follows: IFN-$\gamma$ KO mice, originally made by Dalton et al. (18) and IL-12*p40* KO mice originally made by Magram et al. (19) were purchased from Jackson ImmunoResearch Laboratories. The strains (both on C57BL/6 background) were crossed to generate heterzygotes, who were then crossed again to generate double knockouts. Genomic DNA was extracted from tails of the pups using a Qiagen kit (DNeasy kit), and PCR was used to determine the genotype of individual mice using published primers (18,19). The individual mouse was considered double positive if it was positive for the neomycin gene but negative for both IFN-$\gamma$ and IL-12*p40* genes. Homozygous mice of the desired genotype were used as founders for the double knockout colony. The mice were maintained under specific pathogen-free conditions and bred at the animal facility of the University of Minnesota. For all of the experiments, we used only female mice. All of the studies were reviewed and approved by the Institutional Animal Care and Use Committee of the University of Minnesota.

**Immunization—**We immunized each mouse with AChR purified from the electric organ of *Torpedo californica* as we described previously (20). Briefly, we emulsified 25 $\mu$g of TAChR in 100 $\mu$l of PBS in an equal volume of CFA and used it for multiple s.c. injections along the back of the mouse. We boosted the mice twice, at 4-wk intervals, with the same amount of TAChR in IFA.

**Evaluation of EAMG symptoms—**We measured the strength of the mice sensitized with pancuronium bromide (0.03 mg/kg) by forcing them to hang from an inverted grid. We described this test in detail previously (11,21,22). “Holding time” is the time it took for the mouse to fall three times from the grid. We considered sick mice with holding times shorter than 8.3 min (11,22). The myasthenic nature of the muscular weakness was verified by injecting the mice with edrophonium chloride (0.1 mg/kg, i.p.), a cholinesterase inhibitor that immediately increases the holding time. We tested the mice every 2 wk.

### Proliferation assays

**Proliferation of CD8$^+$-depleted splenocytes—**Twelve weeks after the first immunization, we sacrificed the mice, collected their spleen, and depleted the splenocytes of CD8$^+$ T cells using rat anti-mouse CD8 Ab (BD Biosciences Pharmingen) and paramagnetic beads coated with goat anti-rat IgG (Qiagen), as we described previously (22). We cultured the cells for 3 days in the presence of the following Ag: TAChR (2 $\mu$g/ml); individual synthetic peptides (~20 residues long and overlapped by ~5 residues) spanning the TAChR or mouse AChR $\alpha$ subunit (10 $\mu$g/ml), as described in Refs. 10 and 22. We used Con A (5 $\mu$g/ml; Sigma-Aldrich) as positive control. We determined the basal rate of cell proliferation from cell cultured without any Ag or with a synthetic peptide of a random sequence unrelated to AChR. We determined the rate of cell proliferation from the incorporation of [$^3$H]thymidine, measured by liquid scintillation, and expressed as cpm. When an Ag induced a statistically significant increase in the cell proliferation, we calculated the stimulation index (SI: the ratio between the proliferation of cells cultured in the presence of the Ag and in the presence of the unrelated synthetic peptide). We disregarded SI lower than 2.

**Assessment of the suppressive activity of CD4$^+$CD25$^+$ regulatory T cells—**We immunized WT and dKO mice with TAChR/CFA and after 2 wk boosted them with TAChR/IFA. Within 1 wk after the boost, we collected the mouse splenocytes and used a CD4$^+$CD25$^+$ regulatory T cell isolation kit (Miltenyi Biotec) to purify the following cell

populations: $CD4^+CD25^+$ cells, $CD4^+CD25^-$ cells, and the residual cell population (non-$CD4^+$ cells). The non-$CD4^+$ cells were further depleted of $CD8^+$ cells using rat anti-mouse CD8 Ab and paramagnetic beads coated with goat anti-rat IgG, irradiated (10,000 rad) and used as APC. We cultured 50,000 $CD4^+CD25^-$ cells in U-bottom 96-well plates with 50,000 APC, 1 $\mu$g/ml anti-CD3 mAb (2C11; BD, Pharmingen) as stimulant, and with or without 40,000 $CD4^+CD25^+$ cells, for 72 h at 37°C in 5% $CO_2$. We pulsed the cultures with 1 $\mu$Ci/well of [$^3$H]thymidine for the last 18 h, harvested the cells, and counted the [$^3$H]thymidine that had been incorporated by the cells. We represent the suppressive activity of the $CD4^+CD25^+$ T cells as percentage of inhibition, which is calculated as follows: 100 × (cpm of cultures without $CD4^+CD25^+$ cells − cpm of cultures with $CD4^+CD25^+$ cells)/cpm of cultures without $CD4^+CD25^+$ cells.

### ELISA for the detection of IL-17 in cell culture supernatants

Purified $CD4^+$ T cells ($10^6$/well) and APC from WT and dKO mice immunized twice with TAChR were incubated with TAChR (50 $\mu$g/ml) or Con A or with medium alone in 24-well plates. $CD4^+$ T cells were purified by positive selection using CD4 (L3T4) MicroBeads (Miltenyi Biotec) and were cultured in the presence of $4 \times 10^5$ irradiated APC ($CD8^+$-depleted non-$CD4^+$ cells). After 48 h of incubation at 37°C in 5%$CO_2$, the supernatants were tested for IL-17 using an IL-17 ELISA kit (eBioscience). The samples were tested in a series of dilutions to generate a linear curve. The results were calculated by using the slope of samples divided by the slope obtained in the standard curve expressed in nanograms per milliliter.

### Immunophenotyping of splenocytes

The following anti-mouse Ab were used to characterize the phenotype of splenocytes from naive dKO and WT mice: CD3, CD4, CD8, CD30, NK1.1, CD11c, CD19, IgM (all from BD Pharmingen). The Ab were directly conjugated with FITC or PE. Briefly, the staining was done for 30 min on ice in PBS/0.1% $NaN_3$/1% BSA. The cells were then washed three times, resuspended in PBS, and analyzed. We examined the presence of $CD4^+CD25^+$ regulatory T cells among the mouse spleen $CD4^+$ T cells using PerCP-CD4, PE-CD25, and FITC-forkhead box P3 (FoxP3) triple staining. Specifically, intracellular specific marker Foxp3 was detected using the FITC anti-mouse/rat Foxp3 Staining Set (eBioscience) according to the manufacturer's instruction. Flow cytometry analysis was conducted in a FACScan flow cytometer with CellQuest software (BD Biosciences).

### Measurement of serum anti-AChR Ab

**Radioimmunoprecipitation assay of serum anti-mouse AChR Ab—**As a source of mouse AChR, we used carcasses of WT B6 mice solubilized with Triton X-100 as we described previously (22) and labeled with $^{125}$I-$\alpha$-bungarotoxin ($^{125}$I-$\alpha$BTX). We incubated increasing dilutions of mouse serum with labeled muscle extracts. The complexes of $^{125}$I-$\alpha$BTX mouse AChR and IgG were precipitated using Zysorbin (Zymed Laboratories) and were counted in a 5500 gamma counter (Beckman Coulter). We express the Ab concentration as nanomolar of precipitated $^{125}$I-$\alpha$ BTX binding sites.

**ELISA of anti-TAChR IgG and IgG subclasses—**We used an ELISA that we described previously (10,11) to measure the anti-TAChR total IgG and IgG subclasses (IgG1, IgG2b, and IgG2c) in mouse sera collected 12 wk after the first immunization. Briefly, sera were diluted up to 1/4000 and added to ELISA plates (Nalge Nunc) previously coated with 5 $\mu$g/ml TAChR in coating buffer (10 mM $NaHCO_3$, pH 9.6). As a detecting system, we used HRP-conjugated goat anti-mouse IgG (Sigma-Aldrich) or the appropriate biotinylated anti-mouse IgG subclass Ab (BD Biosciences Pharmingen) followed by avidin-HRP (Sigma-Aldrich). The developing solution was made with equal volumes of 2,2′-azino-di (3-ethylbenzthiazoline-6-

sulfonate)-peroxidase substrate and $H_2O_2$ (Kirkegaard & Perry Laboratories). We measured the absorbance at 405 nm with an ELx800 automated microplate reader (Bio-Tek Instruments). For each sample, we calculated the serum concentration of IgG, IgG1, IgG2b, and IgG2c (expressed as micrograms per milliliter) by comparing the slope of the curve obtained for the sample and the slope obtained for the standard curve. Because purified anti-TAChR IgG or IgG subclasses are not available, we constructed standard curves using purified mouse IgG, IgG1, IgG2a, and IgG2b. The standard curves are not ideal, yet they allowed the comparison of results obtained in different experiments.

### Studies on the NMJ

**Mouse muscle AChR content—**Mouse AChR was extracted from mice carcasses as described previously (23). Briefly, 1 g of muscle taken from each individual carcass was homogenized and solubilized with 1.5% Triton X-100 in 0.05 M Tris buffer. The AChR content was determined using the $^{125}$I-$\alpha$BTX-binding assay we described previously (23,24). We expressed the concentration of muscle AChR as picomoles of $^{125}$I-$\alpha$BTX binding sites per gram of muscle.

**IgG and complement at the NMJ by immunofluorescence microscope—**Mouse hind limb muscle tissue, frozen in liquid nitrogen and stored at −70°C, was embedded in Tissue-Tek OCT compound (Miles Laboratories) and sectioned in the transverse direction into 10-$\mu$m sections using a Jung Frigout 2800E Kryostat (Leica). For each mouse, we analyzed 4–10 muscle sections. We incubated the sections at room temperature in PBS for 10 min and then for 1 h with biotin-conjugated goat anti-mouse IgG polyclonal Ab (Sigma-Aldrich) in PBS containing 2% BSA. We washed the sections three times with PBS and stained them for 1 h at room temperature with Texas Red-labeled $\alpha$BTX (Molecular Probes), FITC-labeled goat anti-mouse C3 Ab (Nordic Immunological Laboratories), and AMCA-S-labeled streptavidin (Molecular Probes). We washed the sections three times with PBS and viewed them in a fluorescence microscope (Nikon Eclipse E800; Nikon). We collected digital images using the program Image Pro Plus (Media Cybernetics,).

**Statistical analysis—**We used repeated measure ANOVA (StatView 5.0.1; Abacus Concepts) and a two-tailed Student's *t* test (Excel; Microsoft). We considered a difference significant when $p < 0.05$.

## Results

### dKO and WT mice develop EAMG symptoms with similar frequency and severity

In three independent experiments, we immunized dKO mice ($n$ = 10, 10, and 13, respectively) and WT mice ($n$ = 9, 6, and 11, respectively) with TAChR/CFA and boosted them twice with TAChR/IFA 4 wk apart. We tested the mouse muscle strength every 2 wk. Fig. 1*A* illustrates the frequency of EAMG weakness (i.e., holding times of 8.3 min or less) among the WT and dKO mice used in the three experiments, about 2 wk after the first and second TAChR/IFA boost. In agreement with the results of previous studies (5,10), the frequency of EAMG weakness differed among experiments: yet, in each experiment, it was the same in the dKO and the WT group. Fig. 1*B* depicts the holding times of all of the individual mice used in the three experiments: 38% of the WT mice and 42% of the dKO mice had EAMG symptoms after the first boost and almost 69% of the mice of both groups had EAMG weakness after the second boost.

### dKO and WT mice have comparable and reduced muscle AChR content

We sacrificed the mice after the second boost (12 wk after the first TAChR immunization) and we measured their muscle AChR content. In all experiments, the WT and the dKO mice had

similar concentrations of muscle AChR, which in most mice were reduced as compared with those of eight naive WT mice that we used as controls. Fig. 2 shows the concentration of muscle AChR (expressed as picomoles per gram of tissue) of the individual WT and dKO mice used in the three experiments and of eight control naive WT mice. Both WT and dKO mice had significantly less muscle AChR than the naive WT mice ( $p = 0.042$ and $p = 0.0052$, respectively).

### dKO and WT mice had IgG and complement at the NMJ

TAChR-immunized IL-12/IL-23$^{-/-}$ mice had IgG, but not complement at the NMJ, suggesting that ineffective synthesis of complement-fixing anti-AChR Ab contributes to their EAMG resistance (11). We examined whether simultaneous absence of IL-12/IL-23 and IFN-$\gamma$ restored the mouse ability to synthesize anti-muscle AChR Ab that fix complement. We determined the presence of IgG and complement at the NMJ of TAChR-immunized mice using specific fluorescent Ab. We analyzed muscle sections from four WT mice and four dKO mice (two mice for each group from those used in experiments 1 and 2), sacrificed after the second boost, 12 wk after the first TAChR injection. Naive WT mice served as negative controls. For each mouse, we analyzed 20 –28 sections. The results we obtained were consistent in all sections, for all of the mice we examined: WT and dKO mice had both IgG and the C3 complement component at the NMJ, identified by the presence of AChR. Fig. 3 shows the results of representative sets of sections.

### dKO mice had less serum anti-TAChR IgG and IgG subclasses than WT mice, but comparable concentrations of anti-mouse muscle AChR Ab

We collected sera 12 wk after the first TAChR immunization from the mice used in experiments 1 and 2. We used ELISA to measure the concentration of anti-TAChR IgG and IgG subclasses. We obtained similar results for both experiments (reported together in Fig. 4). dKO mice had significantly less anti-TAChR IgG and all IgG subclasses than WT mice. They had virtually no anti-TAChR IgG2c and little anti-TAChR IgG1 and IgG2b.

We used radioimmunoprecipitation assays to measure the anti-mouse AChR Ab in those sera. In both experiments, several mice from both the dKO and the WT groups had measurable anti-muscle AChR Ab in the serum (Fig. 5). The WT mice had serum anti-muscle AChR Ab somewhat more frequently than dKO mice, but the difference was not significant.

### CD8$^+$-depleted splenocytes from dKO mice had much reduced proliferative responses to TAChR and TAChR peptides than CD8$^+$-depleted splenocytes from WT mice, yet they responded to several mouse AChR peptides recognized by WT mice

We used CD8$^+$-depleted splenocytes from mice sacrificed 12 wk after the first TAChR immunization to test their proliferative response to the TAChR and to overlapping peptides spanning the TAChR $\alpha$ subunit sequence. We conducted two independent proliferation assays using cells from mice of the first experiment and one using cells from mice of the second experiment and obtained consistent results. The TAChR-induced proliferative responses of dKO mice, although significant, were consistently weaker that those of WT mice. CD8$^+$-depleted splenocytes of WT mice recognized several peptide sequences of the TAChR $\alpha$ subunit ($\alpha$55–74, $\alpha$106 –126, $\alpha$146 –169, $\alpha$181–200, $\alpha$215–249, $\alpha$346 –378, and $\alpha$406 – 423), which included sequences previously identified as immunodominant epitopes in B6 mice ($\alpha$111–126, $\alpha$146 –169, $\alpha$180 –200, $\alpha$346 –368, see Refs. 20,22,25, and 26). In contrast, CD8$^+$-depleted splenocytes from dKO mice responded to TAChR peptides poorly and recognized only the immunodominant peptides $\alpha$111–126, $\alpha$146 –161, and $\alpha$346 –364. Fig. 6 shows representative results.

We used $CD8^+$-depleted splenocytes from mice sacrificed 12 wk after the first TAChR immunization to test their proliferative response to synthetic peptides spanning the sequence of the mouse muscle AChR $\alpha$ subunit (22). We conducted two independent experiments: Fig. 7 shows their results. We observed small yet significant responses to a few peptides for both WT and dKO mice. The intensity of the peptide-elicited responses was of the same order of magnitude for cells from WT and dKO mice. Both strains recognized peptides within the sequence regions $\alpha$191–235 and $\alpha$414 – 433. WT mice, but not dKO mice, recognized also peptide $\alpha$276 –295.

### Similar TAChR-induced production of IL-17 in cultures of $CD4^+$ T cells from TAChR-immunized dKO mice and WT mice

We used cultures of purified spleen $CD4^+$ T cells plus APC from TAChR-immunized dKO and WT mice to determine their ability to secrete IL-17 when restimulated with TAChR in vitro. We found that the TAChR-induced secretion of IL-17 was slightly higher in WT mice, but the difference was not significant ($p > 0.05$). In contrast, the nonspecific IL-17 production induced in vitro by stimulation with Con A was significantly higher for the $CD4^+$ T cells from WT mice than from the dKO mice. Fig. 8 shows the IL-17 concentrations, in nanograms per milliliter, in supernatants of cell cultures from individual dKO or WT mice.

### Naive dKO mice have fewer NK, NK T cells, and $CD4^+CD25^+$ FoxP3 Treg cells than WT mice

To determine whether genetic absence of both IL-12/IL-23 and IFN-$\gamma$ grossly affected the development of $CD4^+$ or $CD8^+$ T cells, or B cells, or dendritic cells, or NK and NK T cells, or of the potentially regulatory $CD4^+$ $CD25^+$ T cell subset (27,28), we analyzed splenocytes from naive dKO and WT mice for the presence of the following surface markers, individually or in the appropriate combinations as indicated: CD3, CD4; CD3, CD8; CD3, CD30 (the latter as an indicator of activation of T cells); CD3, NK1.l; NK1.1, CD11.c (a marker of dendritic cells); CD4, CD25; and CD19, IgM. To determine the presence of $CD4^+CD25^+$ Treg cells, we used a triple fluorescence staining of Foxp3 (a specific marker of $CD4^+CD25^+$ regulatory T cells) coupled with surface staining for CD4 and CD25: *A* of Fig. 9 shows the results of an individual representative experiment done with this approach. This is a more sensitive and specific approach for detection of $CD4^+CD25^+$ regulatory T cells than assessment of the CD25 expression (29). Fig. 9*B* depicts a summary of the results of those experiments: each column represents the average of results obtained in several individual mice ($n = 3–12$). Spleen of naive dKO and WT mice contained comparable concentrations of $CD4^+$ T cells, $CD8^+$ T cells, activated T cells, B cells, and dendritic cells. In contrast, dKO mice had significantly fewer NK (2.68%), NKT cells (1.06%), and $CD4^+CD25^+$ FoxP3 Treg cells (15.99%) than WT mice (4.49% for NK, 3.3% for NKT, and 17.97% for $CD4^+CD25^+$ FoxP3 Treg cells). We obtained similar results when testing the frequency of $CD4^+CD25^+$ FoxP3 Treg cells in dKO mice and WT mice after three TAChR immunizations (data not shown).

### $CD4^+CD25^+$ T cells from dKO mice had less suppressive function than $CD4^+CD25^+$ T cells from WT mice

We determined the ability of $CD4^+CD25^+$ Treg cells from naive and TAChR-immunized dKO or WT mice to inhibit the anti-CD3 Ab-induced proliferation of $CD4^+CD25^-$ T cells T cells from the same mice. We conducted five independent experiments using $CD4^+CD25^+$ Treg cells from TAChR-immunized WT and dKO mice and four experiments using $CD4^+CD25^+$ Treg cells from naive WT and dKO mice. In each experiment, we set up four to six cultures for each of the conditions tested. When stimulated with anti-CD3 mAb in the absence of $CD4^+CD25^+$ T cells, cultures of $CD4^+CD25^-$ T cells (50,000 cells plus 50,000 APC) from WT mouse cells proliferated more strong than the cells from dKO mice. The range of $[^3H]$ thymidine incorporation (expressed as cpm per well) varied in the different experiments: it was

5,290 cpm to 148,693 cpm in the different experiments that used WT cells and 3,700 cpm to 11,538 cpm in the different experiments that used dKO cells. After TAChR immunization, $CD4^+CD25^+$ Treg cells from dKO mice inhibited the proliferation of $CD4^+$ T cells significantly less ( $p = 0.02$) than the $CD4^+CD25^+$ T cells from WT mice. In contrast, the suppressive ability of $CD4^+CD25^+$ Treg cells of naive dKO and WT mice was comparable. Fig. 10 illustrates the average of the results obtained in all of the individual experiments we conducted.

## Discussion

Several studies have shown that Th1 cells and Th1-driven, complement-fixing anti-AChR Ab are important in the development of mouse EAMG (e.g., see Refs. 8,14, and 22). However, the role of IFN-$\gamma$ is still unclear (11–13). In this study, we show that B6 mice are susceptible to EAMG in the absence of IFN-$\gamma$, IL-12, and IL-23, which are the main differentiation and effector cytokines of Th1 cells (9,11). dKO mice immunized with TAChR/CFA-IFA developed modest and much lower Ab and $CD4^+$ T cell responses to the xenogeneic TAChR than WT mice (Figs. 4 and 6). Yet, dKO mice presented EAMG symptoms (Fig. 1) and developed an autoimmune response against mouse AChR that involved both $CD4^+$ T cells and Ab-producing B cells: 1) they had a reduced muscle AChR content, comparable to that of WT mice (Fig. 2); 2) their sera contained anti-mouse AChR Ab in concentrations comparable to those of WT mice (Fig. 5); and 3) the $CD4^+$ T cell responses against peptide sequences of mouse AChR $\alpha$ subunit were similar in dKO and WT mice (Fig. 7). Both dKO and WT mice recognized peptide 215–235, which is immunodominant in B6 mice (22) most strongly and consistently. In one of the two experiments we conducted, mice of both strains recognized also peptide 203–218, which overlaps the immunodominant region 215–235, and peptide 414 – 433, which is frequently recognized by mice of the B6 background after TAChR immunization. WT mice recognized also peptide 191–207, which overlaps peptide 203–218, recognized by both strains, and peptide 276 –296, which was not recognized by dKO mice. Recognition of both of these peptides by $CD4^+$ T cells of B6 mice with EAMG has been described previously (22). The present finding that $CD4^+$ T cells of dKO mice recognized a more limited set of AChR peptides than WT mice is well explained by a less efficient spreading (22) of the repertoire of the autoimmune anti-mouse AChR $CD4^+$ T cells in the combined absence of IL-12/IL-23 and IFN-$\gamma$, because of the resulting lesser efficiency of APC in dKO mice than in WT mice.

The modest intensity of the anti-TAChR response of dKO mice even after multiple TAChR immunizations in CFA-IFA, and the seemingly paradoxical ability of such a low response to trigger a pathogenic autoimmune response to mouse AChR, suggests that absence of IL-12/IL-23 and IFN-$\gamma$ might have impaired the sensitization/differentiation and/or function of both the $CD4^+$ T and B cells that cooperate in the xenogeneic anti-TAChR response and perhaps that of $CD4^+CD25^+$ Treg cells that curb the progression of the anti-TAChR response to involve the mouse AChR. Without an efficient activation of Treg cells, the modest sensitization of pathogenic $CD4^+$ T cells and the IL-12-independent synthesis of complement-fixing anti-AChR Ab that occur in IL-12/IL-23-deficient mice (11) might trigger a pathogenic, self-sustaining anti-muscle AChR response and result in the appearance of EAMG symptoms.

$CD4^+CD25^+$ Treg cells play a key role in maintaining peripheral tolerance to self-Ag (30). Their activity reduced in several experimental autoimmune diseases and human autoimmune diseases (30,31). IFN-$\gamma$ is important for activation and differentiation of $CD4^+CD25^+$ Treg cells (32–34). Mice genetically deficient in STAT1, a mediator of intracellular IFN-$\gamma$ signaling, were more susceptible to EAE than WT mice and had a reduced number and functional impairment of $CD4^+CD25^+$ Treg cells (32). After immunization with collagen, mice genetically deficient in IFN-$\gamma$ were more susceptible to collagen-induced arthritis: they had fewer $CD4^+CD25^+$ Treg cells than WT mice and their $CD4^+CD25^+$ Treg cells had impaired suppressive activity (33). MG patients may have a functional impairment of thymic

$CD4^+CD25^+$ Treg cells (35). Moreover, the number of circulating $CD4^+CD25^+$ Treg cells in MG patients increased after thymectomy, and the increase correlated with the symptom improvement (36).

Both naive and TAChR-immunized dKO mice had slightly but significantly fewer $Foxp3^+C25^+CD4^+$ Treg cells than WT mice (Fig. 9 and data not shown). Moreover, after TAChR immunization, $CD4^+CD25^+$ Treg cells from dKO mice had a significantly less suppressive ability than $CD4^+CD25^+$ Treg cells from WT mice (Fig. 10), suggesting that in our system the decreased suppressive activity of $CD4^+CD25^+$ Treg in dKO mice is not due to the absence of IFN-$\gamma$ only, but it is probably an effect of a combination of factors.

Other mechanisms could be involved in the EAMG susceptibility of dKO mice. Naive dKO mice had significantly fewer NK and NKT cells in their spleen than WT mice (Fig. 9). NK cells facilitate EAMG induction (37): their reduced number is not likely related to the EAMG susceptibility of dKO mice. In contrast, NKT cells may have a role in immunoregulation and in the maintenance of self-tolerance (38,39). Thus, their reduction in dKO mice might contribute to the development of an autoimmune response to mouse AChR after TAChR immunization. In addition, a recent study demonstrated that $\alpha$-galactosylceramide-activated NKT cells control the function of $CD4^+CD25^+$ Treg cells: mice treated with $\alpha$-galactosylceramide had an increased number and suppressive function of $CD4^+CD25^+$ Treg cells (40). The decreased number of NKT cells in dKO mice might contribute to the reduced activity of their $CD4^+CD25^+$ Treg cells.

The recently discovered Th17 $CD4^+$ T cell subset, an independent lineage from the Th1 and the Th2 cells, seems to be responsible for the autoimmune responses that occur in several experimental models of autoimmunity, such as collagen-induces arthritis, EAE (2,14) and experimental autoimmune encephalomyelitis (D. Luger and R. R. Caspi, submitted for publication). The present observations, that TAChR-specific $CD4^+$ T cells obtained from TAChR-immunized dKO and WT mice secrete similar levels of IL-17 when stimulated in vitro with TAChR (Fig. 8), indicate that an effective anti-TAChR sensitization of Th17 cells occurs in dKO mice. IL-23, which is also absent in dKO mice, has a role in maintaining the established Th17 responses (41), but it is not needed for the sensitization and differentiation of Th17 cells. This could explain how Th17 cells can differentiate, and could play a pathogenic role in EAMG of dKO mice, even if this observation is inconsistent with other findings (3,42,43).

The present results indicate that in EAMG, an Ab-mediated experimental autoimmune disease, Th1 cytokines, although important for development of autoimmune diseases, are not the exclusive players. Other mechanisms, such as those mediated by Th17 could have a role in both T cell- and Ab-mediated autoimmunity: they might become more obvious in situations when the Th1 cell function is impaired, as in the dKO mice we used here.

## References

1. Kolls JK, Linden A. Interleukin-17 family members and inflammation. Immunity 2004;21:467– 476. [PubMed: 15485625]
2. Komiyama Y, Nakae S, Matsuki T, Nambu A, Ishigame H, Kakuta S, Sudo K, Iwakura Y. IL-17 plays an important role in the development of experimental autoimmune encephalomyelitis. J Immunol 2006;177:566 –573. [PubMed: 16785554]
3. Veldhoen M, Hocking RJ, Atkins CJ, Locksley RM, Stockinger B. TGF$\beta$ in the context of an inflammatory cytokine milieu supports de novo differentiation of IL-17-producing T cells. Immunity 2006;24:179 –189. [PubMed: 16473830]
4. Sakaguchi S. Naturally arising Foxp3-expressing $CD25^+CD4^+$ regulatory T cells in immunological tolerance to self and non-self. Nat Immunol 2005;6:345–352. [PubMed: 15785760]

5. Conti-Fine, BM.; Protti, M.; Bellone, M.; Howard, JF. Myasthenia Gravis: The Immunobiology of an Autoimmune Disease. R. G. Landes; Austin, TX: 1997.
6. Conti-Fine, BM.; Diethem-Okita, B.; Ostlie, N.; Wang, W.; Milani, M. Myasthenia Gravis and Related Disorders. Humana; Totowa, NJ: 2003. Immunopathogenesis of myasthenia gravis; p. 53-92.
7. Berman PW, Patrick J. Experimental myasthenia gravis: a murine system. J Exp Med 1980;151:204 –223. [PubMed: 7350247]
8. Lennon VA, Lindstrom JM, Seybold ME. Experimental autoimmune myasthenia: a model of myasthenia gravis in rats and guinea pigs. J Exp Med 1975;141:1365–1375. [PubMed: 1127382]
9. Moiola L, Galbiati F, Martino G, Amadio S, Brambilla E, Comi G, Vincent A, Grimaldi LM, Adorini L. IL-12 is involved in the induction of experimental autoimmune myasthenia gravis, an antibody-mediated disease. Eur J Immunol 1998;28:2487–2497. [PubMed: 9710226]
10. Wang W, Ostlie NS, Conti-Fine BM, Milani M. The susceptibility to experimental myasthenia gravis of $STAT6^{-/-}$ and $STAT4^{-/-}$ BALB/c mice suggests a pathogenic role of Th1 cells. J Immunol 2004;172:97–103. [PubMed: 14688314]
11. Karachunski PI, Ostlie NS, Monfardini C, Conti-Fine BM. Absence of IFN-$\gamma$ or IL-12 has different effects on experimental myasthenia gravis in C57BL/6 mice. J Immunol 2000;164:5236 –5244. [PubMed: 10799884]
12. Balasa B, Deng C, Lee J, Bradley LM, Dalton DK, Christadoss P, Sarvetnick N. Interferon$\gamma$ (IFN-$\gamma$) is necessary for the genesis of acetylcholine receptor-induced clinical experimental autoimmune myasthenia gravis in mice. J Exp Med 1997;186:385–391. [PubMed: 9236190]
13. Zhang GX, Xiao BG, Bai XF, van der Meide PH, Orn A, Link H. Mice with IFN-$\gamma$ receptor deficiency are less susceptible to experimental autoimmune myasthenia gravis. J Immunol 1999;162:3775–3781. [PubMed: 10201893]
14. Nakae S, Nambu A, Sudo K, Iwakura Y. Suppression of immune induction of collagen-induced arthritis in IL-17-deficient mice. J Immunol 2003;171:6173– 6177. [PubMed: 14634133]
15. Rohn TA, Jennings GT, Hernandez M, Grest P, Beck M, Zou Y, Kopf M, Bachmann MF. Vaccination against IL-17 suppresses autoimmune arthritis and encephalomyelitis. Eur J Immunol 2006;36:2857–2867. [PubMed: 17048275]
16. Veldhoen M, Stockinger B. TGF$\beta$1, a "Jack of all trades": the link with pro-inflammatory IL-17-producing T cells. Trends Immunol 2006;27:358 –361. [PubMed: 16793343]
17. Cua DJ, Sherlock J, Chen Y, Murphy CA, Joyce B, Seymour B, Lucian L, To W, Kwan S, Churakova T, et al. Interleukin-23 rather than interleukin-12 is the critical cytokine for autoimmune inflammation of the brain. Nature 2003;421:744 –748. [PubMed: 12610626]
18. Dalton DK, Pitts-Meek S, Keshav S, Figari IS, Bradley A, Stewart TA. Multiple defects of immune cell function in mice with disrupted interferon-$\gamma$ genes. Science 1993;259:1739 –1742. [PubMed: 8456300]
19. Magram J, Connaughton SE, Warrier RR, Carvajal DM, Wu CY, Ferrante J, Stewart C, Sarmiento U, Faherty DA, Gately MK. IL-12-deficient mice are defective in IFN $\gamma$ production and type 1 cytokine responses. Immunity 1996;4:471– 481. [PubMed: 8630732]
20. Bellone M, Ostlie N, Lei SJ, Wu XD, Conti-Tronconi BM. The I-Abm12 mutation, which confers resistance to experimental myasthenia gravis, drastically affects the epitope repertoire of murine $CD4^+$ cells sensitized to nicotinic acetylcholine receptor. J Immunol 1991;147:1484 –1491. [PubMed: 1715360]
21. Karachunski PI, Ostlie NS, Okita DK, Conti-Fine BM. Prevention of experimental myasthenia gravis by nasal administration of synthetic acetylcholine receptor T epitope sequences. J Clin Invest 1997;100:3027–3035. [PubMed: 9399949]
22. Ostlie N, Milani M, Wang W, Okita D, Conti-Fine BM. Absence of IL-4 facilitates the development of chronic autoimmune myasthenia gravis in C57BL/6 mice. J Immunol 2003;170:604 – 612. [PubMed: 12496449]
23. Karachunski PI, Ostlie NS, Okita DK, Conti-Fine BM. Interleukin-4 deficiency facilitates development of experimental myasthenia gravis and precludes its prevention by nasal administration of $CD4^+$ epitope sequences of the acetylcholine receptor. J Neuroimmunol 1999;95:73– 84. [PubMed: 10229117]

24. Monfardini C, Milani M, Ostlie N, Wang W, Karachunski PI, Okita DK, Lindstrom J, Conti-Fine BM. Adoptive protection from experimental myasthenia gravis with T cells from mice treated nasally with acetylcholine receptor epitopes. J Neuroimmunol 2002;123:123–134. [PubMed: 11880157]
25. Bellone M, Ostlie N, Lei S, Conti-Tronconi BM. Experimental myasthenia gravis in congenic mice: sequence mapping and H-2 restriction of T helper epitopes on the $\alpha$ subunits of *Torpedo californica* and murine acetylcholine receptors. Eur J Immunol 1991;21:2303–2310. [PubMed: 1680694]
26. Infante AJ, Thompson PA, Krolick KA, Wall KA. Determinant selection in murine experimental autoimmune myasthenia gravis: effect of the bm12 mutation on T cell recognition of acetylcholine receptor epitopes. J Immunol 1991;146:2977–2982. [PubMed: 1707927]
27. Crispin JC, Vargas MI, Alcocer-Varela J. Immunoregulatory T cells in autoimmunity. Autoimmun Rev 2004;3:45–51. [PubMed: 15003187]
28. McHugh RS, Shevach EM, Thornton AM. Control of organ-specific autoimmunity by immunoregulatory $CD4^+CD25^+$ T cells. Microbes Infect 2001;3:919 –927. [PubMed: 11564440]
29. Ziegler SF. Foxp3: of mice and men. Annu Rev Immunol 2006;24:209 –226. [PubMed: 16551248]
30. Beissert S, Schwarz A, Schwarz T. Regulatory T cells. J Invest Dermatol 2006;126:15–24. [PubMed: 16417213]
31. Sakaguchi S, Sakaguchi N, Asano M, Itoh M, Toda M. Immunologic self-tolerance maintained by activated T cells expressing IL-2 receptor $\alpha$-chains (CD25): breakdown of a single mechanism of self-tolerance causes various autoimmune diseases. J Immunol 1995;155:1151–1164. [PubMed: 7636184]
32. Nishibori T, Tanabe Y, Su L, David M. Impaired development of $CD4^+CD25^+$ regulatory T cells in the absence of STAT1: increased susceptibility to autoimmune disease. J Exp Med 2004;199:25–34. [PubMed: 14699080]
33. Kelchtermans H, De Klerck B, Mitera T, Van Balen M, Bullens D, Billiau A, Leclercq G, Matthys P. Defective $CD4^+CD25^+$ regulatory T cell functioning in collagen-induced arthritis: an important factor in pathogenesis, counter-regulated by endogenous IFN-$\gamma$. Arthritis Res Ther 2005;7:R402–R415. [PubMed: 15743488]
34. Sawitzki B, Kingsley CI, Karim OVM, Herber M, Wood KJ. IFN-$\gamma$ production by alloantigen-reactive regulatory T cells is important for their regulatory function in vivo. J Exp Med 2005;201:1925–1935. [PubMed: 15967822]
35. Balandina A, Lecart S, Dartevelle P, Saoudi A, Berrih-Aknin S. Functional defect of regulatory $CD4^+CD25^+$ T cells in the thymus of patients with autoimmune myasthenia gravis. Blood 2005;105:735–741. [PubMed: 15454488]
36. Sun Y, Qiao J, Lu CZ, Zhao CB, Zhu XM, Xiao BG. Increase of circulating $CD4^+CD25^+$ T cells in myasthenia gravis patients with stability and thymectomy. Clin Immunol 2004;112:284 –289. [PubMed: 15308122]
37. Shi FD, Wang HB, Li H, Hong S, Taniguchi M, Link H, Van Kaer L, Ljunggren HG. Natural killer cells determine the outcome of B cell-mediated autoimmunity. Nat Immunol 2000;1:245–251. [PubMed: 10973283]
38. Godfrey DI, Kronenberg M. Going both ways: immune reglation via CD1d-dependent NKT cells. J Clin Invest 2004;114:1379 –1388. [PubMed: 15545985]
39. Margalit M, Ilan Y. Induction of immune tolerance: a role for natural killer T lymphocytes? Liver Int 2005;25:501–504. [PubMed: 15910485]
40. Liu R, La Cava A, Bai XF, Jee Y, Price M, Campagnolo DI, Christadoss P, Vollmer TL, Van Kaer L, Shi FD. Cooperation of invariant NKT cells and $CD4^+CD25^+$ T regulatory cells in the prevention of autoimmune myasthenia. J Immunol 2005;175:7898 –7904. [PubMed: 16339525]
41. Aggarwal S, Ghilardi N, Xie MH, de Sauvage FJ, Gurney AL. Interleukin-23 promotes a distinct CD4 T cell activation state characterized by the production of interleukin-17. J Biol Chem 2003;278:1910 –1914. [PubMed: 12417590]
42. Bettelli E, Carrier Y, Gao W, Korn T, Strom TB, Oukka M, Weiner HL, Kuchroo VK. Reciprocal developmental pathways for the generation of pathogenic effector TH17 and regulatory T cells. Nature 2006;441:235–238. [PubMed: 16648838]

43. Mangan PR, Harrington LE, O'Quinn DB, Helms WS, Bullard DC, Elson CO, Hatton RD, Wahl SM, Schoeb TR, Weaver CT. Transforming growth factor-$\beta$ induces development of the Th17 lineage. Nature 2006;441:231–234. [PubMed: 16648837]

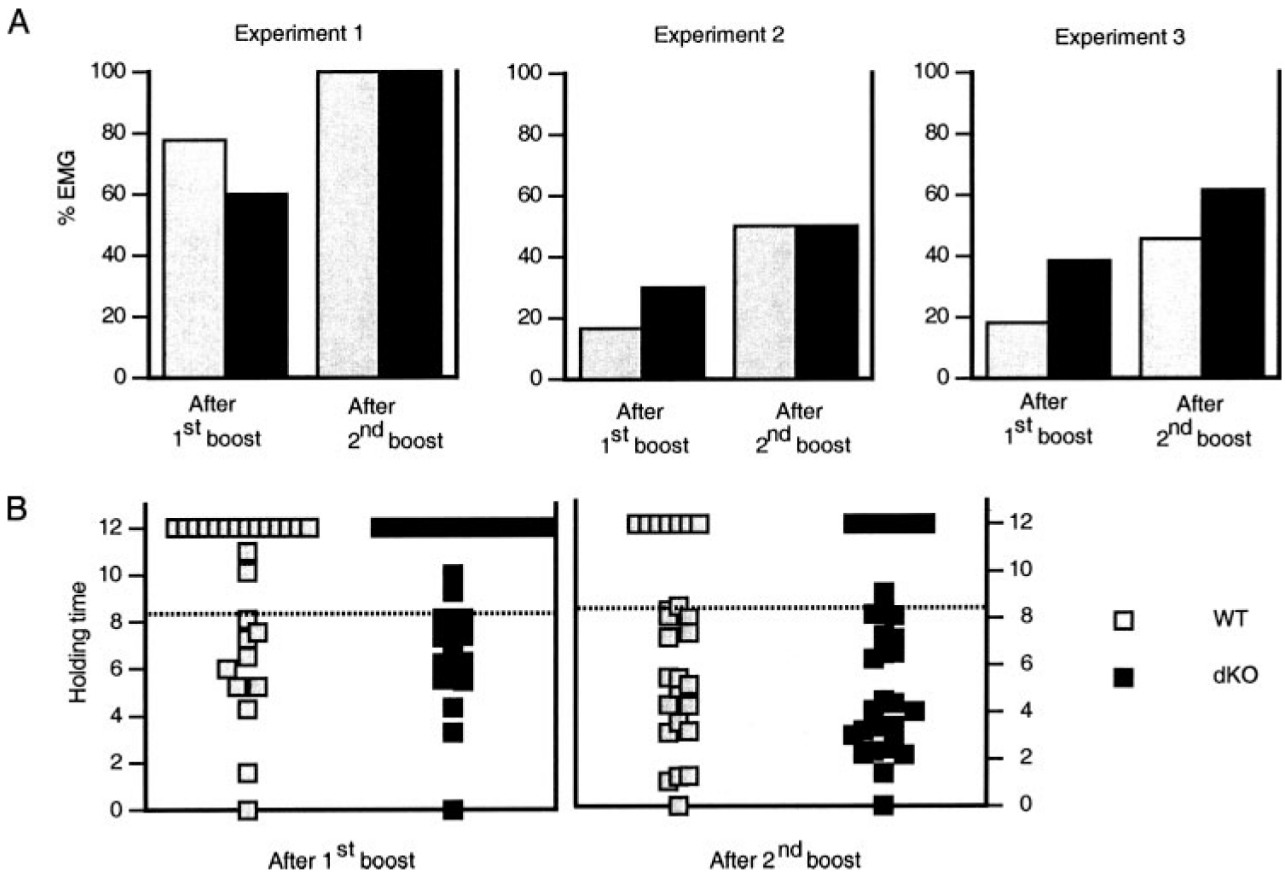


**FIGURE 1.**

EAMG symptoms in TAChR-immunized dKO and WT mice. *A*, Frequency of EAMG weakness among the WT and dKO mice used in three independent experiments evaluated about 2 wk after the first and second TAChR/IFA boost. *B*, Holding times of all individual mice of experiments 1, 2, and 3. The dotted line indicates the holding time of 8.3 min, above which the mouse is considered healthy. EAMG symptoms were always comparable in dKO and WT mice. See text for experimental details.

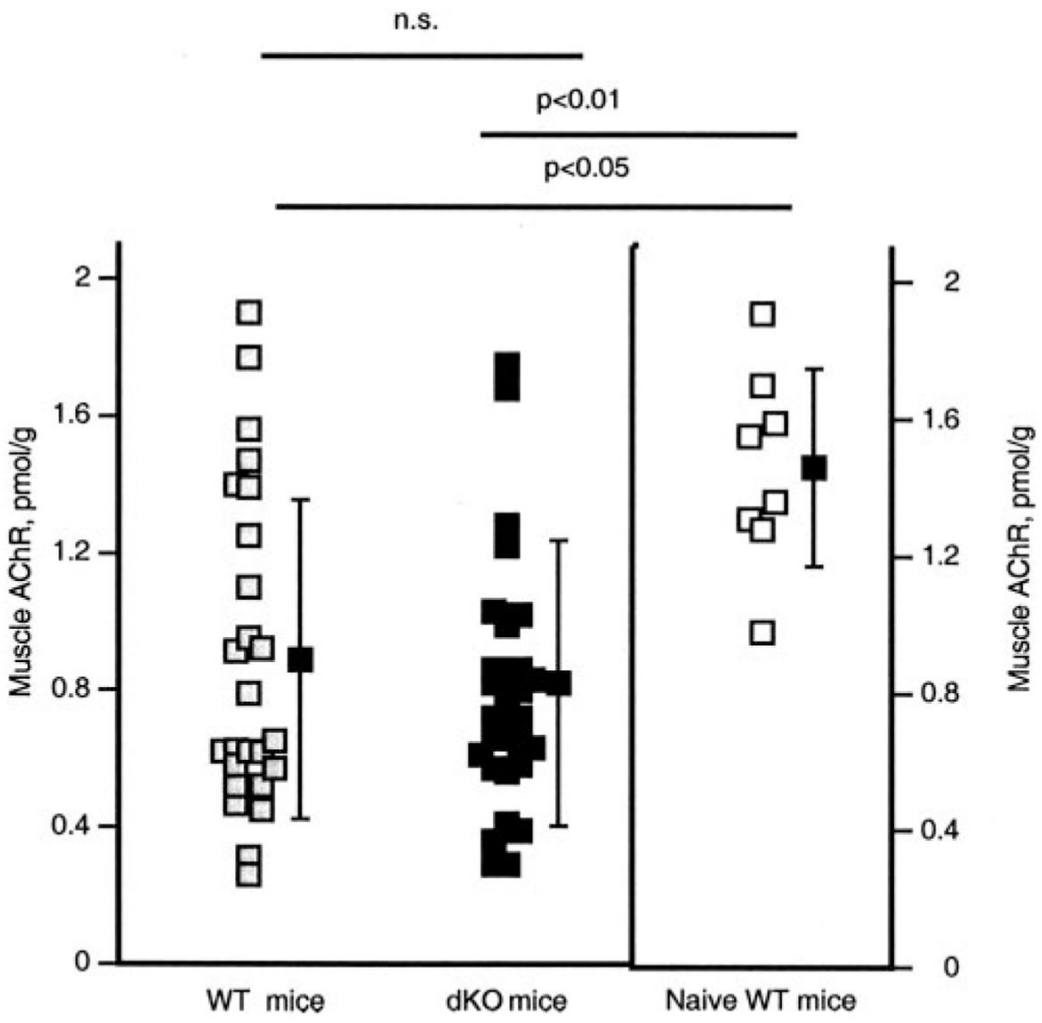


**FIGURE 2.**

Muscle AChR content in TAChR-immunized dKO, WT mice, and naive WT mice. Concentration (picomoles per gram) of AChR in the muscle of individual dKO and WT mice sacrificed 12 wk after the first immunization and of 8 naive WT mice. The filled symbol next to each group represents the group's average concentration ± SD. TAChR-immunized dKO and WT mice had comparable AChR muscle concentrations that were significantly lower than those of naive WT mice. See text for experimental details.

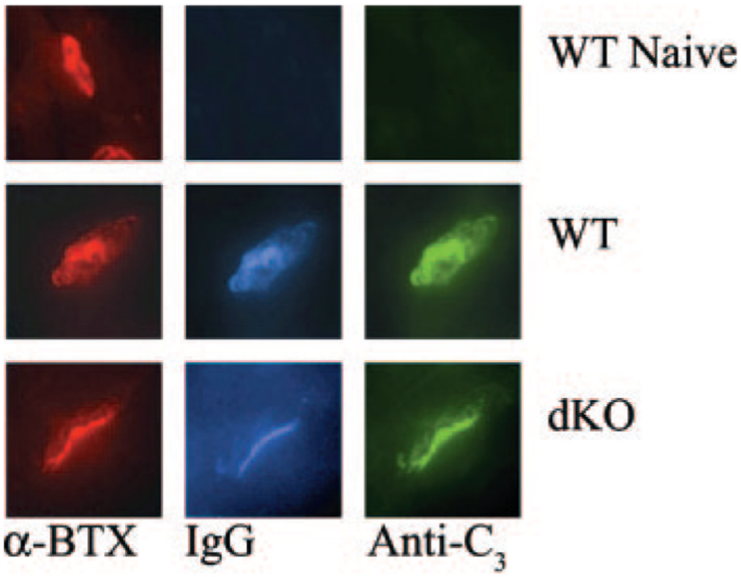


**FIGURE 3.**

Presence of IgG bound to complement at the NMJ of TAChR-immunized dKO, WT, and of naive WT mice. Mice were sacrificed 12 wk after the first TAChR immunization; 20 –28 sections per mouse were analyzed for the presence of AChR (red fluorescence), C3 (blue fluorescence), and IgG (green fluorescence) at the NMJ. Shown is one representative section. Both TAChR-immunized dKO and WT mice had IgG and C3 bound to the AChR at the NMJ. Naive WT mice only stained for the AChR and were negative for both IgG and C3. See text for experimental details.

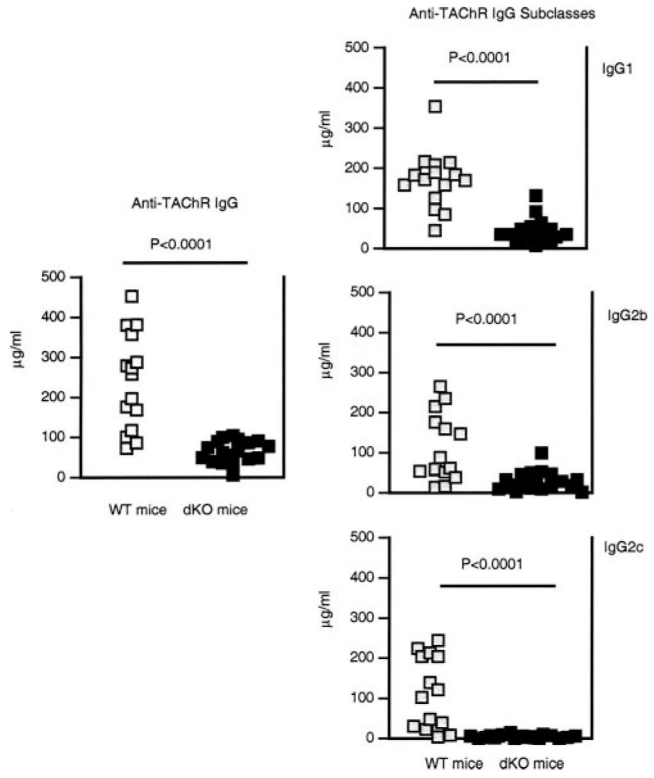


**FIGURE 4.**

Anti-TAChR IgG and IgG subclasses in the sera of TAChR-immunized dKO and WT mice. Concentrations (micrograms per milliliter) of anti-TAChR IgG, IgG1, IgG2b, and IgG2c in the individual sera of dKO and WT mice of experiments 1 and 2 were tested by ELISA. Sera were collected 12 wk after the first TAChR immunization. dKO mice had significantly less anti-TAChR IgG and IgG subclasses than WT mice. See text for experimental details.

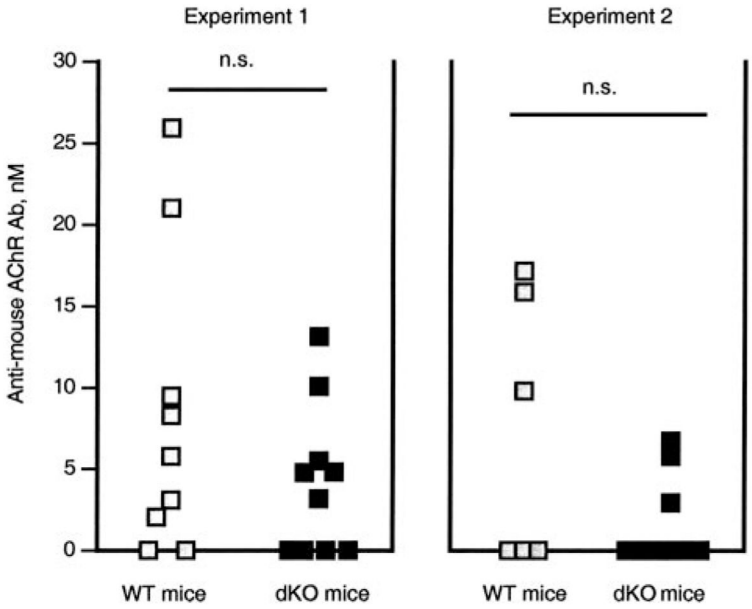


**FIGURE 5.**

Anti-mouse AChR Ab in the sera of TAChR-immunized dKO and WT mice. Concentrations (nanomolar) of anti-mouse AChR Ab in the individual sera of dKO and WT mice of experiments 1 and 2. Sera were collected 12 wk after the first TAChR immunization. WT mice had serum anti-mouse AChR Ab more frequently than dKO, but the difference between the concentrations was not significant. See text for experimental details.

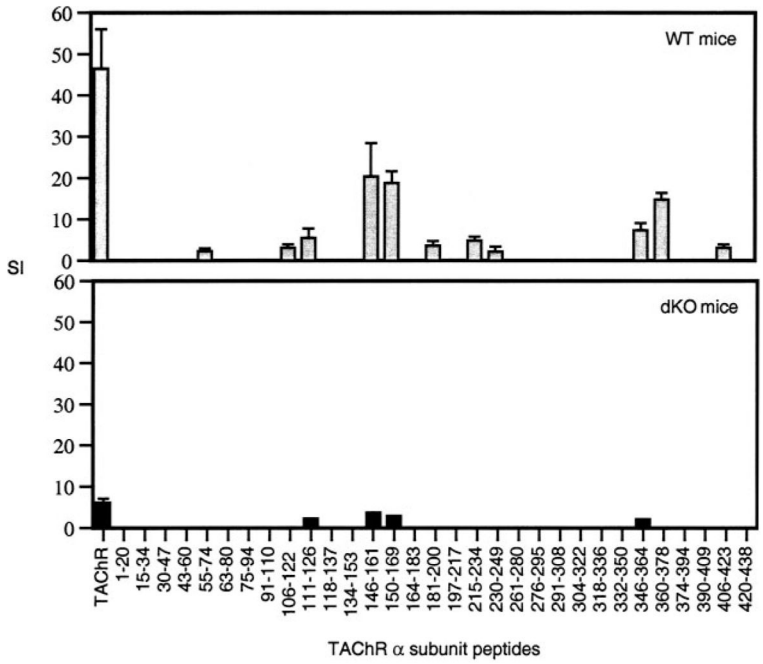


**FIGURE 6.**

Proliferative response of $CD8^+$-depleted splenocytes obtained from TAChR-immunized dKO and WT mice against peptides spanning the $\alpha$ subunit of the TAChR. $CD8^+$-depleted splenocytes obtained from dKO and WT mice 12 wk after the first TAChR immunization were cultured in the presence of peptides spanning the $\alpha$ subunit of TAChR or with TAChR. The columns of the plots represent the SI ± SD calculated with the cpm of quadruplicated cultures (one of three consistent proliferation assays). The background cpm of cells incubated with an unrelated peptide as stimulant were 342.5 + 81.5 for WT mice and 980.17 + 202.28 for dKO mice. $CD8^+$-depleted splenocytes of WT mice responded to a higher number of peptides and more vigorously than dKO mice. Although with different intensity, both dKO and WT mice responded to peptides sequences previously identified as immunodominant epitopes in B6 mice. See text for experimental details.

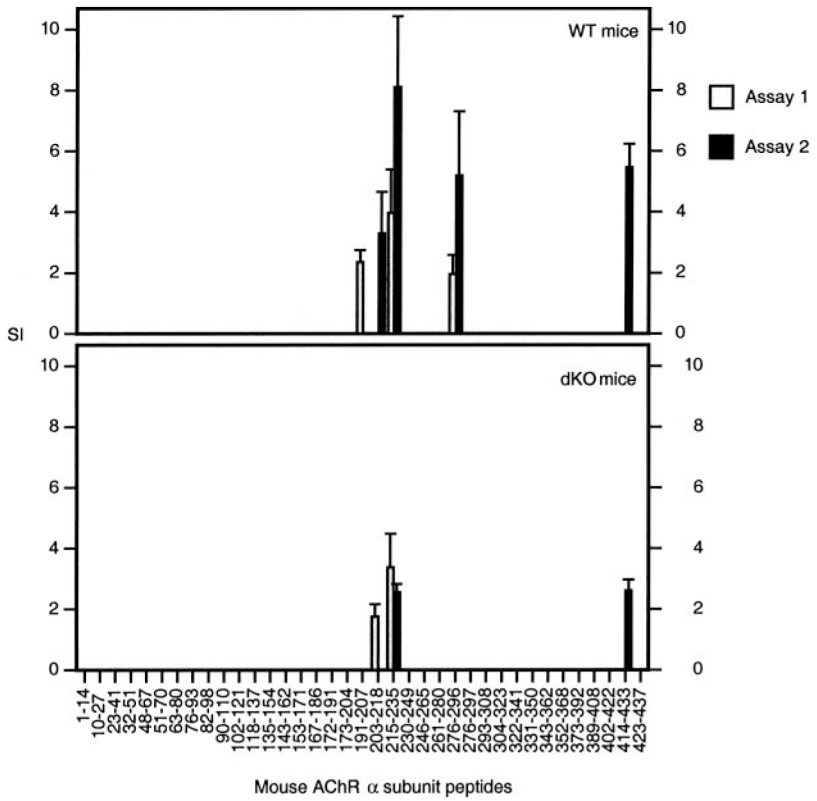


**FIGURE 7.**

Proliferative response of $CD8^+$-depleted splenocytes obtained from TAChR-immunized dKO and WT mice against peptides spanning the $\alpha$ subunit of the mouse AChR. The columns of the plots represent the SI ± SD of two proliferation assays conducted with $CD8^+$ depleted splenocytes obtained from dKO and WT mice 12 wk after the first TAChR immunization. Assay 1 is represented by light gray columns and assay 2 by dark gray columns. Both dKO and WT mice responded to few peptides and their response was of the same order of magnitude. Both WT and dKO mice recognized peptides within the sequence $\alpha$191–235 and $\alpha$414 – 433. WT mice, but not dKO mice, recognized also peptide $\alpha$276 –295. See text for experimental details.

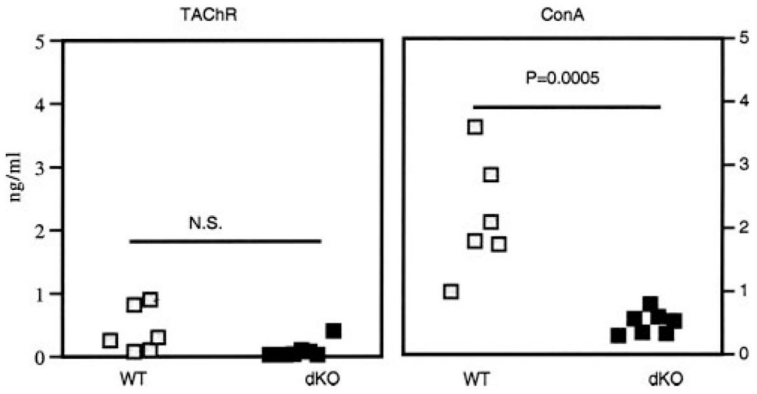


**FIGURE 8.**

IL-17 concentration in the supernatant of purified $CD4^+$ splenocytes obtained from TAChR-immunized WT and dKO mice stimulated by TAChR or Con A. $CD4^+$ T cells from TAChR-immunized WT mice ($n = 6$) and TAChR-immunized dKO mice ($n = 7$) were isolated and incubated with Ag and APC for 48 h, then the supernatants were harvested and tested by ELISA. Each dot represents the results obtained from each individual mouse. The amount of specific IL-17 production induced by TAChR stimulation is comparable in the two strains of mice. The nonspecific production stimulated by Con A is significantly higher in WT mice than in dKO mice. See text for experimental details.

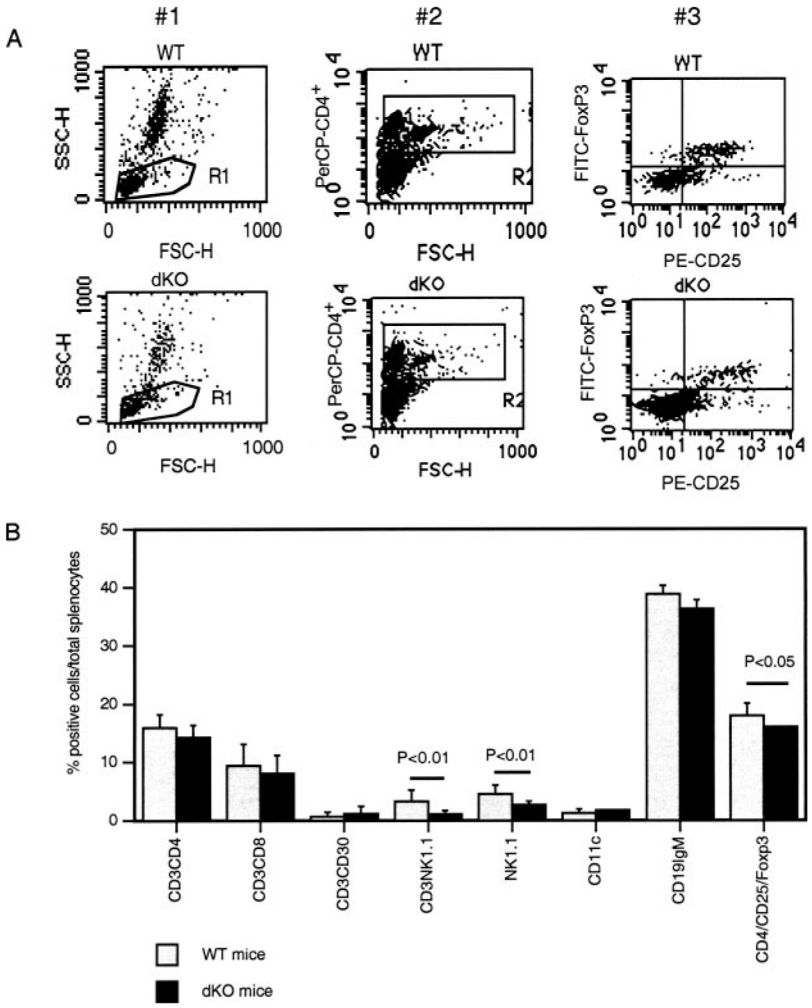


**FIGURE 9.**

Phenotype of splenocytes obtained from naive dKO and WT mice. *A*, The results of a representative flow cytometry analysis done with whole spleen cells stained with PerCP-CD4, FITC-FoxP3, and PE-CD25. In plot #1, R1 is the gate defining the population of interest, in plot #2 R2 is the gate defining the $CD4^+$ cells. The *right upper quadrant* of plot #3 shows the cells positive for the three markers used. The average of all of the triple staining we performed is represented in *B* (CD4/CD25/Foxp3). *B*, The phenotype of splenocytes obtained from several individual mice (three to eight mice). dKO mice had significantly less NK, NKT, and $CD4^+CD25^+Foxp3^+$ T cells than WT mice. See text for experimental details.

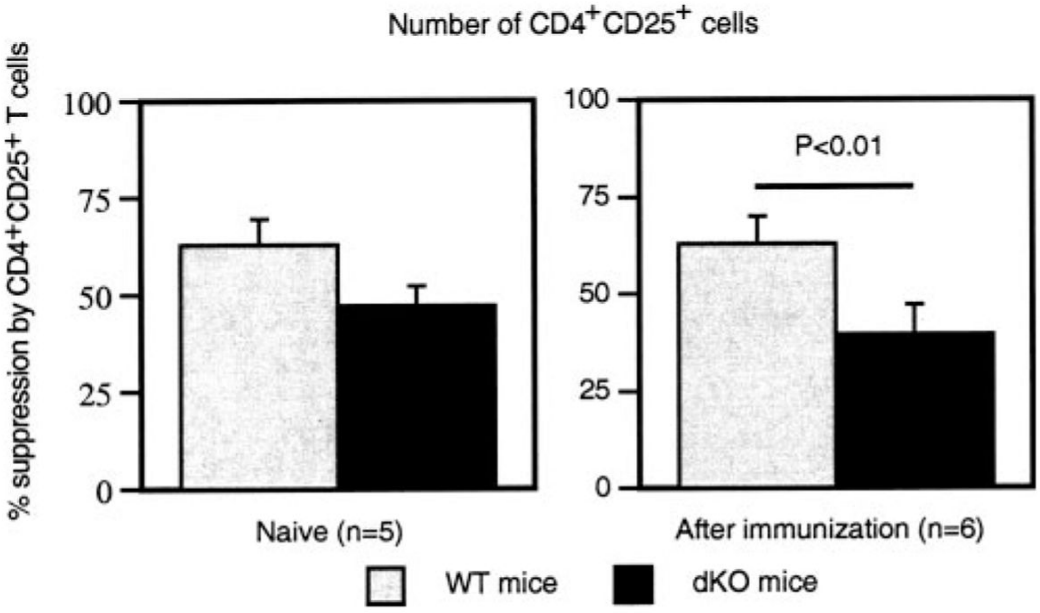


**FIGURE 10.**

Suppressive activity of $CD4^+CD25^+$ Treg cells obtained from TAChR-immunized dKO and WT mice. The columns represent the average ± SD of the percentage of suppression obtained in five to six independent experiments as indicated. $CD4^+CD25^+$ Treg cells from TAChR-immunized dKO mice inhibited the anti-CD3-induced proliferation of $CD4^+CD25^-$ T cells significantly less ($p = 0.02$) than $CD4^+CD25^+$ Treg cells from TAChR-immunized WT mice. The suppressive ability of $CD4^+CD25^+$ Treg cells from naive dKO and WT mice was comparable. See text for experimental details.